


# Exploring the effects of Danshen-Honghua herb pair on the intestinal flora of rats with acute myocardial ischemia and its microbial transformation in vitro

Zhi-Peng Xue<sup>1</sup>, Hui-Hui Zhou<sup>1</sup>, Chen Huan<sup>2</sup>, Ning Wang<sup>1</sup>, Jing Li<sup>1</sup>, Yi Meng<sup>1</sup>, Yi-Jun Zhao<sup>1</sup>, Ji-Qing Bai<sup>1</sup>, Yun-Dong Xie<sup>1</sup>, Yuan-Gui Yang<sup>1</sup>, Xiao-Ping Wang<sup>1\*</sup> 

<sup>1</sup>College of Pharmacy, Shaanxi University of Chinese Medicine, Xianyang 712046, China. <sup>2</sup>Department of Medical Technology, Shaanxi University of Chinese Medicine, Xianyang 712046, China.

\*Correspondence to: Xiao-Ping Wang, College of Pharmacy, Shaanxi University of Chinese Medicine, No. 1, Middle Section of Century Avenue, Qindu District, Xianyang 712046, China. E-mail: wangxiaoping323@126.com.

## Author contributions

Xue ZP, Zhou HH, and Wang XP designed this experiments. Xue ZP wrote the article. Zhou HH and Huan C performed in vitro incubation experiments. Zhao YJ and Meng Y processed animal experiment samples. Wang N, Li J, Xie YD, and Yang YG analyzed the data. Wang XP and Bai JQ guided the experiment and provided funding for the research.

## Competing interests

The authors declare no conflicts of interest.

## Acknowledgments

This work was supported by the National Natural Science Foundation of China (CN) (No.81974544).

## Peer review information

Traditional Medicine Research thanks Xiao-Bo Wang and other anonymous reviewers for their contribution to the peer review of this paper.

## Abbreviations

DHHP, Danshen-Honghua herb pair; AMI, acute myocardial ischemic; ISO, isoproterenol; NOR, normal; MOD, model; DH, Danshen-Honghua; HSYA, hydroxysafflor yellow A; HPLC, high performance liquid chromatography.

## Citation

Xue ZP, Zhou HH, Huan C, et al. Exploring the effects of Danshen-Honghua herb pair on the intestinal flora of rats with acute myocardial ischemia and its microbial transformation in vitro. *Tradit Med Res.* 2024;9(4):21. doi: 10.53388/TMR20230726001.

Executive editor: Xi-Yue Liu.

Received: 26 July 2023; Accepted: 29 December 2023;

Available online: 03 January 2024.

© 2024 By Author(s). Published by TMR Publishing Group Limited. This is an open access article under the CC-BY license. (<https://creativecommons.org/licenses/by/4.0/>)

## Abstract

**Background:** The Danshen-Honghua herb pair (DHHP) is a common modern Chinese medicine pair for activating blood circulation and resolving blood stasis. It has been used for centuries to treat cardiovascular and cerebrovascular diseases and is often found in some herbal compounds for treating cardiovascular diseases. The aim of this study was to explore the effects of DHHP on the intestinal flora of rats with acute myocardial ischemia and its microbial transformation in vitro. **Methods:** In this study, we investigated the protective effect of DHHP on isoproterenol-induced acute myocardial ischemia in rats based on metagenomic sequencing technology, and further characterized the in vitro metabolic transformation products of DHHP, so as to investigate its anti-myocardial ischemic efficacy material basis. **Results:** Pharmacodynamic results demonstrated that DHHP significantly ameliorated pathological changes and improved abnormal cardiac enzyme levels in acute myocardial ischemia rats. In addition, metagenomic analysis showed the efficacy of DHHP in ameliorating the isoproterenol-induced modifications of the intestinal flora in rats. Specifically, DHHP promoted the growth of the intestinal potential probiotics such as *Lactobacillus* while suppressing the pathogenic bacteria, including *Escherichia* and *Streptococcus*. The in vitro metabolism results showed that the DHHP's active components underwent primarily phase I metabolism through hydroxylation, decarboxylation, and dehydration inversions in the isolated intestinal flora of acute myocardial ischemia rats and in phase II through sulfation esterification and methylation reactions. **Conclusion:** The results suggest that there may be a bidirectional regulatory effect between DHHP and intestinal flora, which is important to explain the pharmacological mechanism of DHHP.

**Keywords:** Danshen-Honghua herb pair; acute myocardial ischemia; intestinal flora; metagenomic sequencing; in vitro metabolism; HPLC-Q-TOF-MS/MS

**Highlights**

1. Effect of DHHP on the treatment of AMI in rats by regulating the structure of intestinal flora.
2. Active ingredients in DHHP can be metabolized by rat isolated intestinal flora.
3. There are interactions between intestinal flora and drugs.

**Medical history of objective**

DHHP is a pair of medicines commonly used in modern Chinese medicine formulas to invigorate blood circulation and remove blood stasis, which have been clinically proven for hundreds of years. Danshen was first published in *Shennong Bencao Jing* (ShengNong's herbal classic, Unknown author, 1st–2nd centuries A.D.) and Honghua in *Kai Bao Ben Cao* (Liu Han and Ma Jie, 973 A.D.), both of which have the efficacy of invigorating blood circulation and removing blood stasis (Pathological manifestations of slowed blood flow resulting from the blockage of normal blood flow), subduing swelling and relieving pain. It is widely used in the treatment of coronary heart disease, angina pectoris and other ischemic cardiovascular diseases, and its pharmacological effects and clinical efficacy are remarkable.

**Background**

Acute myocardial ischemia (AMI) refers to a set of symptoms caused by insufficient blood flow to the heart, leading to myocardial ischemia and hypoxia due to occlusion of coronary arteries [1]. At present, AMI has become a common non-communicable disease worldwide and is characterized by its sudden beginning, severity, and high mortality rate [2]. According to the theory of Chinese medicine, AMI arises from blood vessels becoming stagnant, causing a reduction in nourishment of the heart vessels and producing pain if they do not function properly. It belongs to the category of chest impedance and heartache in traditional Chinese medicine. Qi (The very subtle substances in the human body, which are highly dynamic and constantly running, are one of the basic substances that make up the human body and maintain its life activities) deficiency and blood stasis is one of the main pathogeneses of chest paralysis and heart pain. Thus, the treatment involves the improvement of Qi and blood flow, resolution of stasis, and alleviation of pain [3, 4]. Numerous studies in Western medicine have established causal connections between myocardial ischemia and various factors, including oxygen radical generation, calcium overload, apoptosis, inflammatory response, and impaired energy metabolism [5].

*Salvia miltiorrhiza* Bge. (Danshen) from the family Labiatae have the effects of activating blood circulation, dispersing bruises, and alleviating swelling and pain [6]. *Carthamus tinctorius* L. (Honghua), from the family Asteraceae can invigorate blood circulation, disperse bruises, and alleviate pain [7]. Modern research showed that the active components in Danshen have the ability to enhance myocardial contraction, regulate heart function, balance myocardial oxygen consumption, dilate coronary arteries, increase blood flow, and anti-inflammatory and scavenging free radicals [8]. The active components found in Honghua have been identified to inhibit apoptosis of cardiomyocytes, reduce oxidative stress damage, enhance impaired energy metabolism, hinder inflammatory reactions, and regulate calcium ions both intracellularly and extracellularly [9]. Danshen and Honghua were commonly used to activate blood circulation and resolve blood stasis, and when combined, they exhibit synergistic effects. These effects are frequently encountered in certain Chinese herbal formulations for cardiovascular and cerebrovascular ailments, such as Danhong Huayu Oral Liquid, Danhong Injection, Xinling Tablets, Linaoxin Capsules, and others [10, 11]. Research has demonstrated that administering the active ingredients found in a combination of Danshen and Honghua not only treats unstable angina pectoris and reduces myocardial injury in rats that undergo myocardial ischemia-reperfusion, but also offers superior protection

for both myocardial and cerebral functions when compared to administering Danshen or Honghua alone [12, 13].

The intestinal flora is commonly referred to as the “second human genome”. It has become a significant area of international research to discover new pathophysiological mechanisms and therapeutic approaches for cardiovascular diseases that utilize the intestinal flora [14]. A range of studies have demonstrated that herbal monomers and compounds are effective in treating coronary heart disease by improving the composition of intestinal flora, producing a variety of beneficial bacteria, reducing harmful bacteria, and minimizing inflammation in the intestines and throughout the body [15–17]. The complex nature of herbal components may result in interactions between multiple components within the body. Considering the complexity of the human body, drug components may also have intricate interactions with it [18]. Therefore, there is an undeniable connection between intestinal flora and drug interactions. The intestinal flora could enhance drug metabolism and convert it into more easily absorbed or higher pharmacologically effective metabolites [19]. Previous research has suggested that the Danshen-Honghua herb pair (DHHP) has protective effects against myocardial ischemic injury in rats. However, certain water-soluble components of the DHHP, including hydroxysafflor-yellow-A (HSYA) and salvianolic acid B, exhibit low absolute oral bioavailability and tend to remain in the intestinal tract [20, 21]. Therefore, we suppose that the anti-myocardial ischemic effect of the DHHP is related to the intestinal flora. In this study, we analyzed the in vitro metabolism of DHHP in rat intestinal flora based on HPLC-Q-TOF-MS/MS and the effect of DHHP on the diversity of intestinal flora in rats with AMI by metagenomic sequencing technology to further investigate the possible mechanism of DHHP in the treatment of AMI. Thus, it is worth investigating the interaction between the DHHP and the intestinal flora of rats.

**Materials and methods****Materials and reagents**

Danshen (*Salvia miltiorrhiza* Bge., root and rhizome) was collected from Heze City, Shandong Province, China. Honghua (*Carthamus tinctorius* L., florets) was collected from Tacheng City, Xinjiang Province, China. Professor Ji-Qing Bai from Shaanxi University of Chinese Medicine authenticated them, and their morphological and chemical authentications were consistent with the standards set by *Pharmacopoeia of the People's Republic of China 2020*. Isoprenaline hydrochloride (ISO) was purchased from Sigma-Aldrich (St. Louis, MO, USA). Chengdu Durst Biotechnology Co., Ltd. (Chengdu, China) provided Salvianolic acid B and Danshensu, while lithospermic acid, rosmarinic acid, and protocatechuic acid were purchased from Jiangxi Baicaoyuan Biotechnology Co., Ltd. (Jiangxi, China). HSYA was purchased from the China Institute for Food and Drug Control (Beijing, China). Gifu anaerobic medium, vitamin K1, and 1.5 mg of hemin were purchased from Qingdao Haibo Biotechnology Co., Ltd. (Qingdao, China).

**Preparation of standard solution and DHHP extract**

About 5 mg each of Danshensu, salvianolic acid B, lithospermic acid, HSYA, and rosmarinic acid were weighed and placed into individual 5 mL volumetric flasks. They were then dissolved in 50% methanol to a constant volume and shaken thoroughly. The standard solutions were analyzed by high performance liquid chromatography (HPLC), and the results are shown in Figure 1A.

Firstly, 600 g danshen and 200 g honghua were accurately weighed, add Danshen to 6,400 mL of water. Soak the mixture at room temperature for 60 minutes. Then add honghua and soak at 50 °C for 120 min, filtrated. Extract the filter residue twice with 8 times the amount of water at 50 °C for 120 minutes each time, and the filtrate was combined and concentrated under reduced pressure to contain 1.44 g of raw herbs per mL, obtained DHHP extracts, determined by HPLC the contents of Danshensu, HSYA, rosmarinic, lithospermic and salvianolic acids B, and the contents were 4.5, 16.8, 1.84, 4.7 and

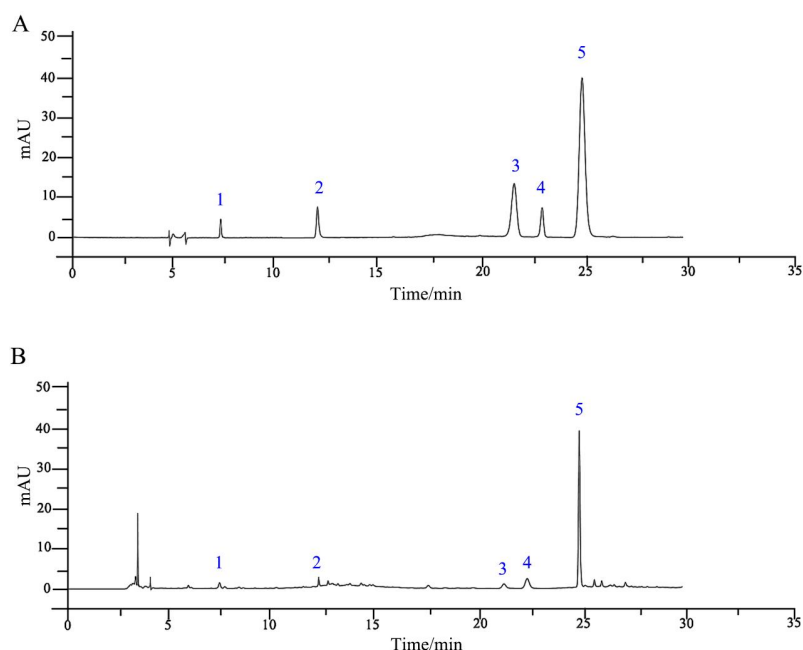


**Figure 1** The HPLC chromatograms of standards and DHHP extracts. (A) Mixed standards. (B) DHHP extracts. 1: Danshensu. 2: hydroxysafflor-yellow-A. 3: Rosmarinic acid. 4: Lithospermic acid. 5: Salvanolic acid B. DHHP, Danshen-Honghua herb pair; HPLC, high performance liquid chromatography.

55.64 mg/g, respectively (Figure 1B).

#### Animal grouping and drug administration

Thirty SPF male Sprague-Dawley (SD) rats (8-week-old, 180–220 g) were obtained from Chengdu Dashuo experimental animal Co., Ltd. (Sichuan, China) (license number: SCXK (Chuan) 2020 – 030), and housed in a temperature controlled ( $25 \pm 5^\circ\text{C}$ ) room at  $45 \pm 5\%$  relative humidity under a consistent lighting cycle (12 h light/dark). This study was conducted by the National Institutes of Health Guide for the Care and Use of Laboratory Animals and was approved by the Laboratory Animal Ethics Committee of Shaanxi University of Traditional Chinese Medicine (ethics approval number SUCMDL20220228001).

SD rats were randomly divided into three groups: a normal group (NOR), a model group (MOD), and a Danshen-Honghua group (DH). The NOR and the MOD group were given water at 1 mL/100 g, and the DH group was given DHHP extracts (4.8 g/kg/d) for 7 days, after 1 h of administration on day 6, except for the NOR group, the other groups were injected subcutaneously ISO (85 mg/kg) for 2 continuous days, established the rat model of AMI.

#### Sample collection

After 12 h following the last injection of ISO, the blood was obtained via the abdominal aorta and centrifuged (3,000 rpm, 15 min, and  $4^\circ\text{C}$ ). The heart was also removed quickly and fixed in a 10 % formaldehyde solution. The contents of the large cecum of rats were removed, rapidly frozen in liquid nitrogen, and stored in a  $-80^\circ\text{C}$  refrigerator.

#### H&E staining

After being fixed in a 10% formaldehyde solution, the rats' hearts were dehydrated using different concentrations of alcohol (75%, 85%, and 95% ethanol, followed by anhydrous ethanol), then embedded in paraffin and sliced into sections. Subsequently, they were cleared of wax, stained with hematoxylin, and subjected to a 1% hydrochloric acid alcohol fractionation followed by rinsing with tap water until blue. The next step was eosin staining, dehydration, and transparency, culminating in sealing and microscopic study of the pathological characteristics of rat myocardium.

#### Biochemical analysis

The serum levels of AST were measured using an Olympus AU-640 automated biochemical analyzer from OLYMPUS OPTICAL Co., Ltd., (Tokyo, Japan), CK-MB and cTnI were determined via an automatic chemiluminescence immunoassay analyzer (Roche Elecsys 2010) from Hoffman Roche Co., Ltd., (Basel, Switzerland).

#### Metagenomic sequencing analysis

Soil DNA Kit was purchased from Omega Bio-Tek (Norcross, GA, America) and used for extraction, and the extracted DNA was assayed. The concentration of DNA was measured using a Qubit 4 fluorometer, while quality control of extracted DNA was ascertained through 1% agarose gel electrophoresis. The DNA samples were fragmented using a Bioruptor machine, with the entire library preparation concluding by implementing steps such as DNA double end repair, A-tail addition, sequencing junction addition, ligand purification, and PCR amplification to enrich the library template. After constructing the libraries, their quantity was measured by Qubit 4. Quality control of the PCR-rich fragments using an Agilent 2100 was used to verify the size and distribution of the DNA libraries. The mixed library (at a concentration of 10 nm) was appropriately diluted and subsequently screened by machine sequencing.

The raw sequencing data were subjected to quality control and host filtering to obtain valid clean data. Next, the reads from all samples were assembled, and gene prediction, species annotation, common functional database annotation, and abundance clustering analysis were performed.

#### Transformation assay in vitro

The anaerobic medium was prepared by weighing 49.0 g of Gifu anaerobic medium in a beaker, adding 1,000 mL of purified water, and dissolving it by heating. After autoclaving it at  $120^\circ\text{C}$  for 25 min, 1 mL of sterile 0.1% vitamin K1 solution and 1 mL of heme chloride (5 mg/mL) were added when cooled to about  $50^\circ\text{C}$ , mixed well, and set aside.

The cecal contents of the experimental rats were mixed with sterile saline in a 1 g:4 mL ratio, placed in a centrifuge tube, and vortexed before being centrifuged. The supernatant was then combined with sterilized anaerobic medium in a ratio of 1:9 mL. After being mixed, the solution was transferred into an anaerobic incubation bag and

incubated for 12 h at 37 °C in a thermostatic incubator to generate an enterobacterial culture solution. The enterobacterial culture solution was placed in a culture flask containing 20 mL; next, 1 mL of DH extract (0.288 g/mL) was added, thoroughly mixed, and separated into three equal samples. These samples were then placed in anaerobic culture bags and incubated in a constant temperature incubator at 37 °C. After 0, 2, 6, 10, 24, and 48 h, samples were collected, and the reactions were halted by adding equal volumes of methanol, followed by vortex centrifugation. The liquid part of the mixture was collected and passed through a microporous membrane that measured 0.22 µm in size, ensuring sterility of the filtration process. Subsequently, the sample was tested using HPLC-Q-TOF/MS for further analysis.

#### Conditions for HPLC-Q-TOF-MS/MS analysis

Chromatographic conditions were employed using a Thermo Hypersil Synchronis C18 column measuring 2.1 mm × 100 mm with 1.7 µm. The mobile phase consisted of a 0.1% formic acid aqueous solution, labelled as A, and an acetonitrile solution, labelled as B. Gradient elution 0 min, 6% B; 0–5 min, 6%–10% B; 5–20 min, 10%–21% B; 20–27 min, 21%–48% B; 27–30 min, 48%–100% B; 30–35 min, 100% B; 35–38 min, 100%–6% B; 38 min, 6% B. The column temperature was 30 °C, the volume flow rate was 0.3 mL/min, and the injection volume was 1 µL.

The mass spectrometry was conducted by means of an electrospray ionization source (ESI) with negative ion mode scanning. The ionization spray voltage was −4,500 V for negative ion mode, and nitrogen was used for the atomization gas and auxiliary gas. The atomization pressure and the auxiliary gas pressure were both set to 50 Pa. The collision voltage was 30 eV. The auxiliary gas was maintained at a temperature of 500 °C, and the gas curtain gas was maintained at 35 °C. A mass scan range of  $m/z$ : 100–2,000 was employed.

#### Statistics analysis

Data were analyzed using GraphPad Prism 8 statistical software, and

experimental data were expressed as the mean ± SD. The data of each group were analyzed by one-way analysis of variance and statistical comparison of differences between groups, and Tukey's multiple comparison test,  $P < 0.05$  as the difference being statistically significant.

#### Results

##### Histopathological examination

The effects of DHHP on the myocardial pathology of rats in the AMI model are shown in Figure 2. The myocardial cells of the NOR group were well-organized with typical myocardial cell morphology, transverse and longitudinal lines, and no observable infiltration of inflammatory cells. In contrast, the MOD group experienced evident myocardial damage, disorganized myocardial fibres, interstitial slackness, congestion, swelling, and a considerable infiltration of inflammatory cells, indicating successful modelling. In the DH group, the myocardial morphology and structure appeared normal, with myocardial fibers exhibiting neat arrangements and minimal edema. Myocardial cell nuclei were uniformly sized, with occasional interstitial swelling noted, suggesting that DHHP improved myocardial injury in rats.

##### Myocardial enzyme test results

AST is a commonly used cardiac enzyme in myocardial tissue. CK-MB is one of the fastest and most obvious cardiac enzymes to rise in myocardial response, and it is an important marker for the diagnosis of AMI. If myocardial tissue is ischemic and hypoxic, cTnI has a high specificity for myocardial injury. In comparison with the NOR group, the levels of AST, CK-MB, and cTnI in the MOD group were significantly higher ( $P < 0.01$ ). On the other hand, the DH group could significantly decrease the activity of AST, CK-MB, and cTnI in serum in comparison to the MOD group ( $P < 0.05$ ,  $P < 0.01$ ) (Figure 3), suggesting that abnormal cardiac enzyme levels were improved by DHHP.

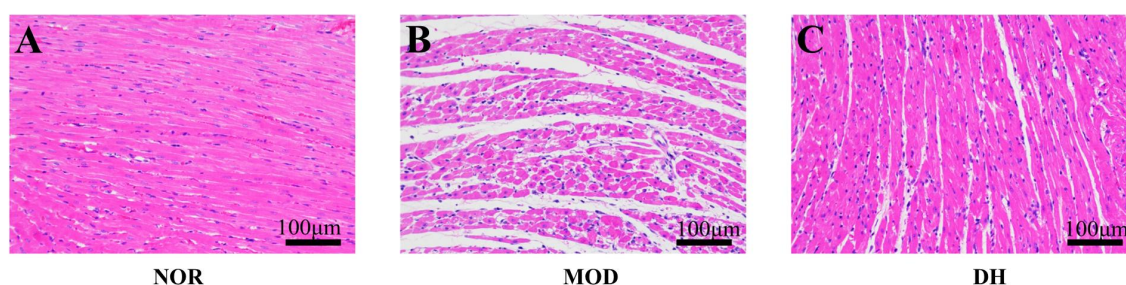


**Figure 2 Photos of myocardial pathology from each group stained with HE (200 ×).** (A) Myocardial pathology of the NOR group stained with HE. (B) Myocardial pathology of the MOD group stained with HE. (C) Myocardial pathology of the NOR group stained with HE. MOD, model; NOR, normal; DH, Danshen-Honghua.

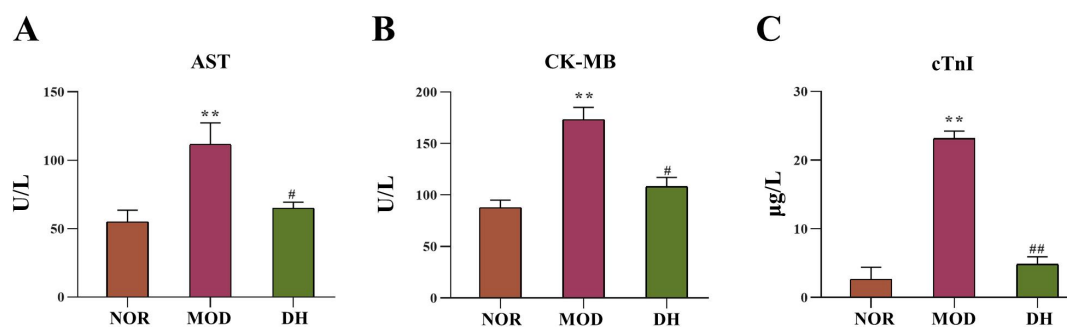


**Figure 3 Myocardial enzyme levels of rat's blood serum in each group.** (A) The contents of AST in the blood serum. (B) The contents of CK-MB in the blood serum. (C) The contents of cTnI in the blood serum. Data were expressed as means ± SD. (n = 6). \* $P < 0.05$ , \*\* $P < 0.01$  vs. NOR group; # $P < 0.05$ , ## $P < 0.01$  vs. MOD group. MOD, model; NOR, normal; DH, Danshen-Honghua; SD, Standard Deviation.



### Species composition analysis of intestinal flora

**Sequencing data quality control results.** A total of 659,771,550 raw sequences and 98,965,732,500 bases were acquired from 9 samples, with an average of 73,307,950 sequences and 10,996,192,500 bases per sample. Subsequently, 656,401,922 high-quality sequences (average length 72,933,547, maximum length 79,784,348, minimum length 66,304,125) were obtained following screening and filtering of raw sequencing data. After collecting valid sequences and removing host contamination, the combined contigs sequence set underwent splicing. Then, the MMseqs2 software was used to de-redund the sequence set, resulting in a non-redundant contigs set comprising 9517215 genes with a total sequence length of 6850113637 bp. The credibility of the results of the species and functional analyses was enhanced by the quality control of the raw data.

**Analysis of intestinal flora variability.** We examined the levels of various species within different phylum and genus groups to evaluate the effects of DHHP on gut dysbiosis. At the level of phylum (Figure

4A), all groups were mainly composed of Bacteroidetes, Proteobacteria, Firmicutes, and Actinobacteria. A total of 206 genera were detected at the genus level, with the top 20 genera displayed in Figure 4B. In the model group, the relative abundance of *Parabacteroides*, *Butyricimonas*, *Odoribacter*, *Escherichia* and *Parasutterella* genera was significantly up-regulated compared to the normal group ( $P < 0.05$ ), suggesting an increase in microbial abundance under AMI. However, the DH group was able to significantly back-regulate the relative abundance of the aforementioned genera at normal levels (Figure 4C).

**PCoA analysis.** In order to evaluate the structural differences between groups of samples at the functional level of KEGG, we performed PCoA analysis. The PCoA analysis displayed in Figure 5 reveals a distinct difference between the NOR group and the MOD group, implying an alteration in the intestinal flora of the model rats. In contrast, the DH group was proximate to the NOR group, suggesting that DHHP modulated the abnormal intestinal flora composition in AMI rats.

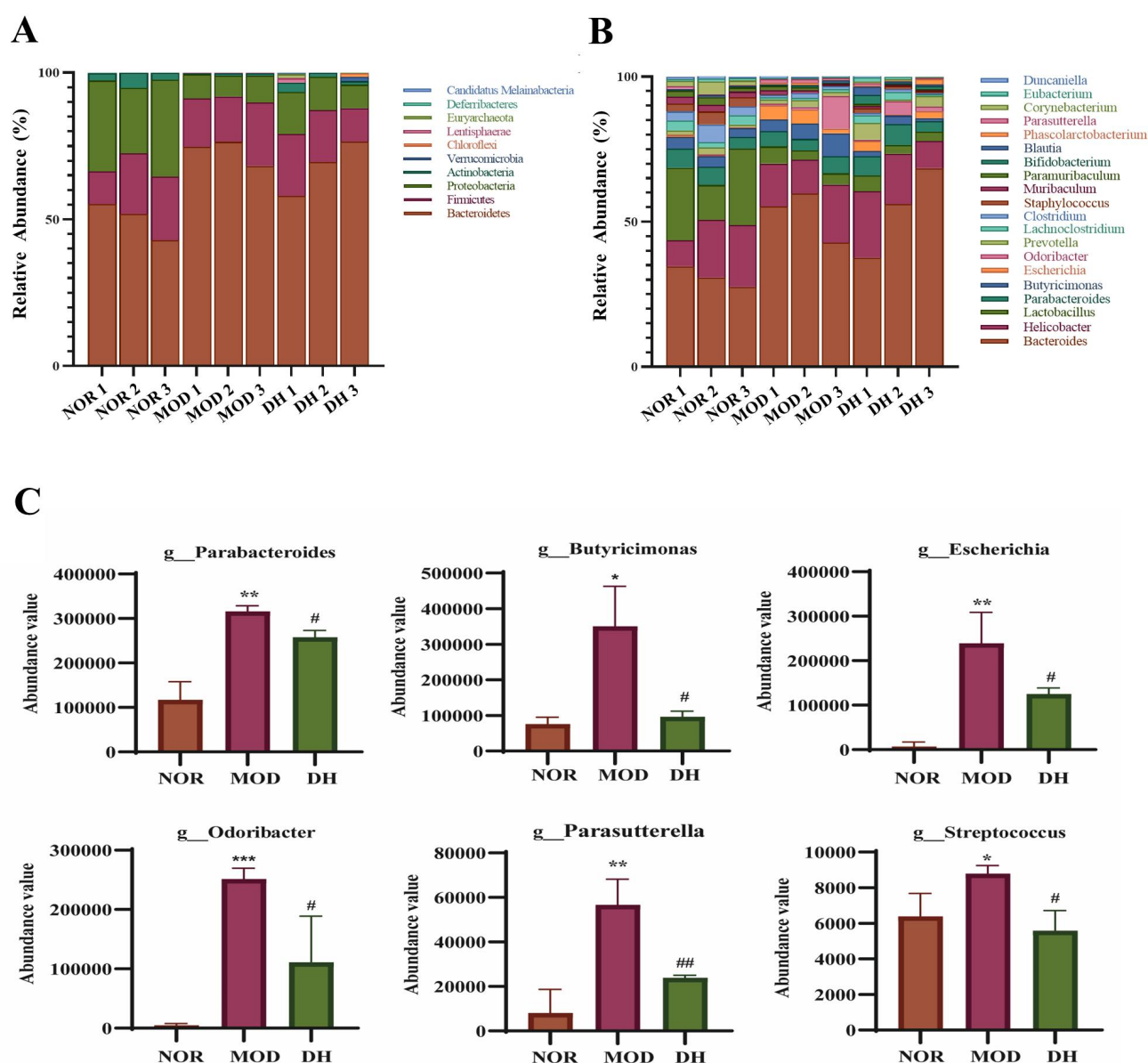


**Figure 4 Structural composition of the intestinal microbial community in each group of rats.** (A) Abundance distribution of intestinal flora at the phylum level. (B) Abundance distribution of intestinal flora at the genus level. (C) Differential analysis of intestinal microorganisms at the genus level. Data were expressed as means  $\pm$  SD. (n = 3). \* $P < 0.05$ , \*\* $P < 0.01$ , \*\*\* $P < 0.001$  vs. NOR group; # $P < 0.05$ , ## $P < 0.01$  vs. MOD group. MOD, model; NOR, normal; DH, Danshen-Honghua; SD, Standard Deviation.

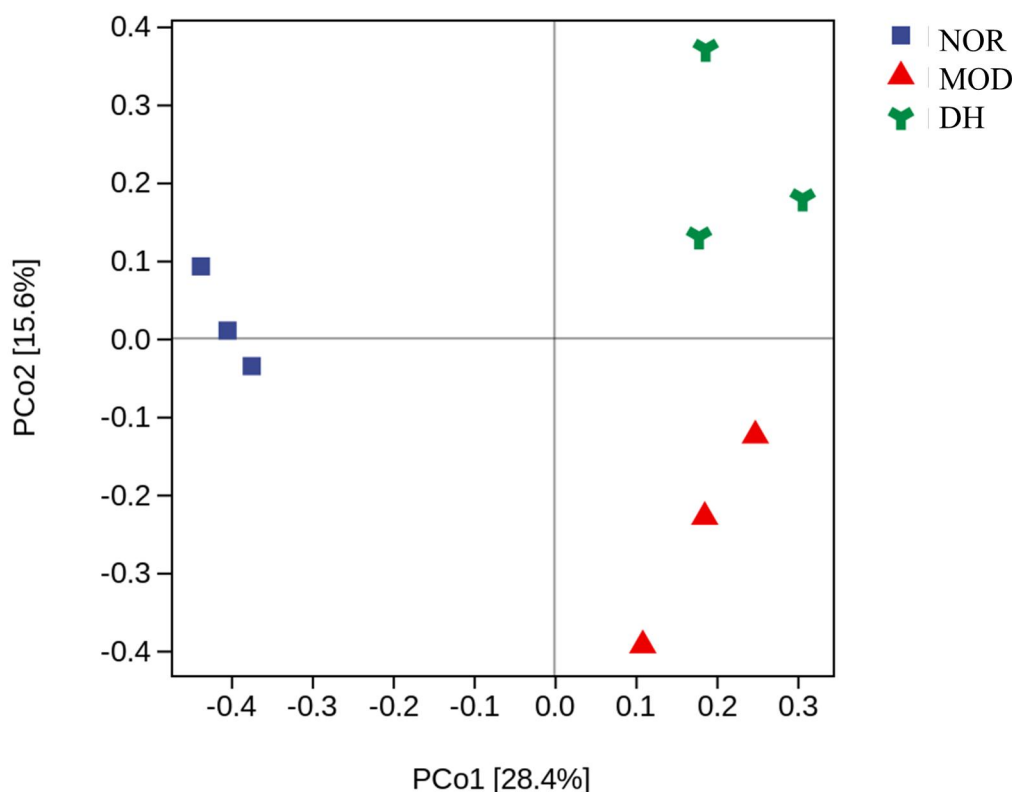


**Figure 5** PCoA analysis of intestinal flora function at the KEGG orthogonal level in the NOR, MOD, and DH groups. KEGG, Kyoto Encyclopedia of Genes and Genomes. MOD, model; DH, Danshen-Honghua; NOR, normal.

#### Functional predictive analysis

Dysregulation of gut microbial composition can cause changes in intestinal flora function. We further investigated the effect of DHHP on intestinal flora function in AMI rats. The primary functions of the three groups of intestinal flora at KEGG1 level are illustrated in Figure 6A. Notably, metabolism exhibits the highest percentage, which suggests a robust correlation between the intestinal flora's functionality and metabolism. Consequently, the primary focus of analysis will center on the metabolic aspects evident in the KEGG3 level pathway, as shown in Figure 6B–6C. These categories include pyruvate metabolism, propanoate metabolism, citrate cycle, butanoate metabolism, and glycerophospholipid metabolism. Additionally, a comparison between the NOR and MOD groups showed that 19 metabolic categories of intestinal flora were significantly enriched with butanoate metabolism, pyruvate metabolism, DNA replication, sterol degradation, and others. The MOD group showed a significant decrease in the relative abundance of Butanoate metabolism, Nucleotide excision repair, and pyruvate metabolism compared to the NOR group ( $P < 0.05$ ). Additionally, the DHHP exhibited a significant regression effect on these metabolisms ( $P < 0.05$ ). This result suggests that the interaction of these metabolic pathways may be an important mechanism by which DHHP regulates rats with AMI.

#### HPLC-Q-TOF-MS/MS analysis

The transformation of the main components of the DHHP in the isolated intestinal flora of rats with AMI was examined by HPLC-Q-TOF-MS/MS (Figure 7), then the metabolites were identified and analyzed.

Based on the information of the secondary mass spectrometry fragments in the negative ion mode, as shown in Table 1 and Table 2, the corresponding compounds were identified, and their possible structures and molecular formulas were inferred by comparing retention times and fragment ion information as well as mass spectral

library searches.

#### Identification and analysis of prototype products of DHHP in the isolated intestinal flora of rats with AMI

The negative mode displayed the excimer ion peak  $[M-H]^-$   $m/z$  197.0463  $C_9H_9O_5$  at 3.52 min retention time for compound M1. Upon comparing the fragment ion  $[M-H-CO_2-H_2O]^-$   $m/z$  135.0458 ( $C_8H_7O_2$ ) with the control, it was confirmed that M1 is Danshensu.

The excimer ion peak  $[M-H]^-$   $m/z$  611.1650  $C_{27}H_{31}O_{16}$  is observed in the negative mode at a retention time of 8.54 minutes for compound M5. The fragment ions  $[M-H-C_4H_8O_4]^-$   $m/z$  491.1211 ( $C_{23}H_{23}O_{12}$ ) and  $[M-H-C_6H_{10}O_5-H_2O-CO]^-$   $m/z$  403.1047 ( $C_{20}H_{19}O_9$ ) are consistent with the HSYA standard, thus identifying compound M5 as HSYA.

At a retention time of 22.87 minutes, rosmarinic acid was confirmed as compound M10, as indicated by the appearance of the excimer ion peak  $[M-H]^-$   $m/z$  359.0745  $C_{18}H_{15}O_8$ , fragment ions  $[M-H-C_9H_9O_3]^-$   $m/z$  197.0460 ( $C_9H_9O_5$ ), and  $[M-H-H_2O-C_9H_9O_3]^-$   $m/z$  179.0350 ( $C_9H_7O_4$ ) in negative mode. Standard rosmarinic acid was used for comparison.

At a retention time of 23.54 minutes, the negative ion mode revealed the presence of an excimer ion peak  $[M-H]^-$   $m/z$  537.1052  $C_{27}H_{21}O_{12}$  and a fragment ion  $[M-H-CO_2-C_9H_{10}O_5]^-$   $m/z$  295.0619 ( $C_{17}H_{11}O_5$ ) of compound M11. Upon comparison with the lithospermic acid standard, compound M11 was identified as lithospermic acid.

The excimer ion peak  $[M-H]^-$   $m/z$  717.1482  $C_{36}H_{29}O_{16}$ , fragment ion  $[M-H-C_9H_{10}O_5]^-$   $m/z$  519.0941 ( $C_{27}H_{19}O_{11}$ ),  $[M-H-C_9H_{10}O_5-C_9H_9O_4]^-$   $m/z$  339.0516 ( $C_{18}H_{11}O_7$ ) appeared in negative mode at  $t_R$  of 24.35 min for compound M14, and compound M14 was identified as salvianolic acid B by comparison with salvianolic acid B standard.

#### Identification and analysis of metabolites of DHHP in the isolated intestinal flora of rats with AMI

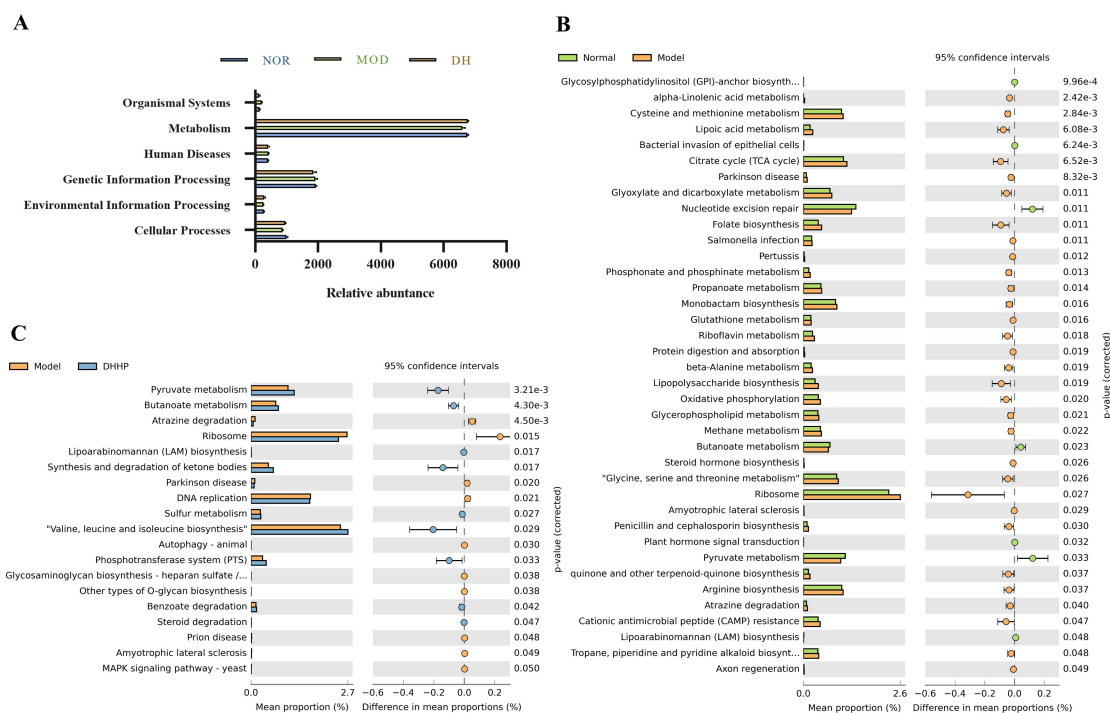


**Figure 6 Functional predictive analysis.** (A) Differential analysis of intestinal microbial function among the three groups of KEGG1. (B) Analysis of the differences in KEGG metabolic pathways between the NOR and MOD groups. (C) Analysis of the differences in KEGG metabolic pathways between the MOD and DH groups. KEGG, Kyoto Encyclopedia of Genes and Genomes; MOD, model; DH, Danshen-Honghua; NOR, normal.

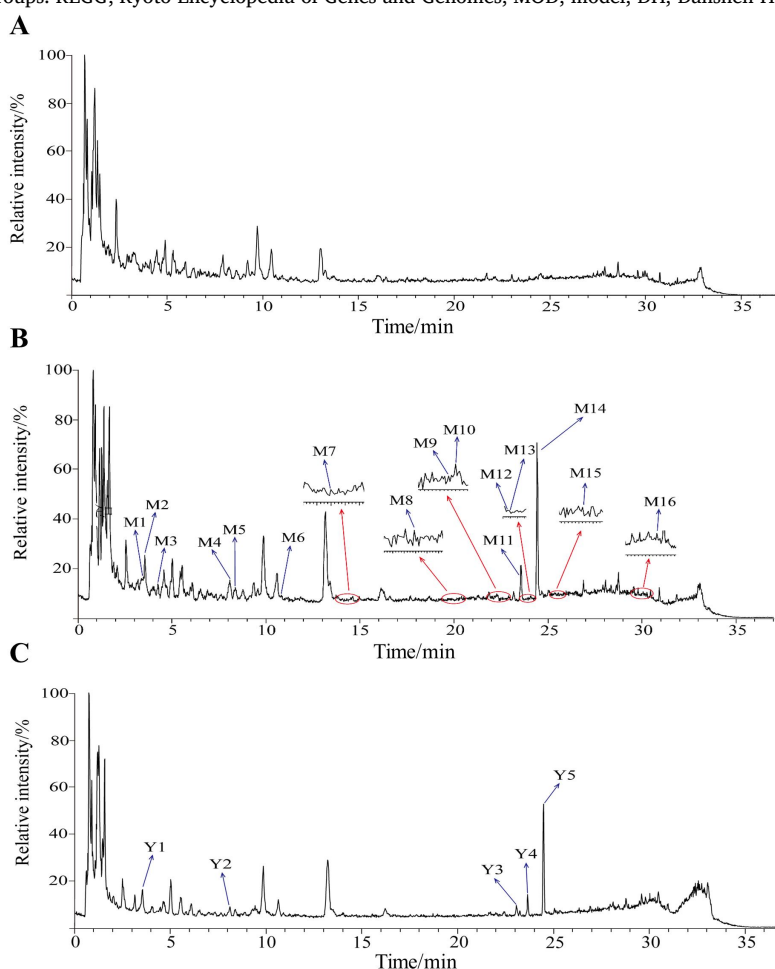


**Figure 7 Base peak chromatograms of prototype components and metabolites of DHHP in intestinal bacteria incubation solution of model rats.** (A) blank enterobacteria solution. (B) 24 h model group incubation sample. (C) Inactivated model group incubation sample. DHHP, Danshen-Honghua herb pair.

**Table 1 Metabolites of DHHP in isolated intestinal bacteria solution of model rats**

No.	t <sub>R</sub> /min	Experimental	Theoretical	Error/ppm	Formula	Fragment ion	Identification
M1 <sup>a</sup>	3.52	197.0463	197.0445	9.13	C <sub>9</sub> H <sub>9</sub> O <sub>5</sub>	135.0458, 123.0457, 109.0297	Danshensu
M2	3.55	395.0949	395.0973	-6.07	C <sub>18</sub> H <sub>19</sub> O <sub>10</sub>	197.0463, 179.0356, 135.0457	Danshensu dimer
M3	4.35	153.0192	153.0202	6.54	C <sub>7</sub> H <sub>5</sub> O <sub>4</sub>	109.0223, 91.0194	Protocatechuic acid
M4	8.07	181.0484	181.0495	-6.19	C <sub>9</sub> H <sub>9</sub> O <sub>4</sub>	135.0457, 121.0302, 109.0301	Deoxydanshensu
M5 <sup>a</sup>	8.54	611.1650	611.1606	7.20	C <sub>27</sub> H <sub>31</sub> O <sub>16</sub>	491.1211, 403.1047, 325.0730	HSYA
M6	10.60	277.0024	277.0012	4.33	C <sub>9</sub> H <sub>9</sub> O <sub>8</sub> S	197.1301, 179.0354	Sulfate danshensu
M7	14.11	551.1176	551.1184	-1.45	C <sub>28</sub> H <sub>23</sub> O <sub>12</sub>	533.1116, 507.1337, 436.2588	Methyl Lithospermic acid
M8	20.51	593.1526	593.1501	4.21	C <sub>27</sub> H <sub>29</sub> O <sub>15</sub>	593.1526, 472.9865, 327.0523, 285.0407	Hydroxy saffron yellow pigment A dehydration product
M9	22.81	245.0117	245.0114	1.22	C <sub>9</sub> H <sub>9</sub> O <sub>6</sub> S	245.0117, 165.0230, 121.0302	Danshinin double dehydroxylation reaction, sulfuric acid esterification binding reaction
M10 <sup>a</sup>	22.87	359.0745	359.0761	-4.46	C <sub>18</sub> H <sub>15</sub> O <sub>8</sub>	197.0460, 179.0354, 161.0248	Rosmarinic acid
M11 <sup>a</sup>	23.54	537.1052	537.1027	4.65	C <sub>27</sub> H <sub>21</sub> O <sub>12</sub>	295.0619, 197.0495, 109.0297	Lithospermic acid
M12	23.55	493.1152	493.1129	4.66	C <sub>26</sub> H <sub>21</sub> O <sub>10</sub>	313.0739, 295.0620, 197.0461	Decarboxylation product of Lithospermic acid
M13	23.59	535.0893	535.0871	4.11	C <sub>27</sub> H <sub>19</sub> O <sub>12</sub>	359.0743, 197.0460, 179.0352, 135.0455, 109.0297	Rosmarinic acid combined with glucuronide
M14 <sup>a</sup>	24.35	717.1482	717.1450	4.46	C <sub>36</sub> H <sub>29</sub> O <sub>16</sub>	519.0941, 339.0516, 321.0412, 295.0618, 197.0459, 135.0456	Salvianolic acid B
M15	25.41	731.1636	731.1607	3.97	C <sub>37</sub> H <sub>31</sub> O <sub>16</sub>	533.1100, 353.0674, 335.0570	Methyl salvianolic acid B
M16	30.03	549.1077	549.1238	7.10	C <sub>25</sub> H <sub>25</sub> O <sub>14</sub>	373.1106, 313.0738, 197.0549, 165.0204, 121.0304	Monoglucuronide monomethylated rosmarinic acid

<sup>a</sup>: Components of the prototype. DHHP, Danshen-Honghua herb pair; HSYA, hydroxysafflor yellow A.

**Table 2 Metabolites of DHHP in inactivated intestinal bacteria solution of model rats**

No.	t <sub>R</sub> /min	Experimental	Theoretical	Error/ppm	Formula	Fragment ion	Identification
Y1 <sup>a</sup>	3.56	197.0462	197.0445	8.63	C <sub>9</sub> H <sub>9</sub> O <sub>5</sub>	135.0460, 123.0456, 109.0297	Danshensu
Y2 <sup>a</sup>	8.75	611.1639	611.1606	5.40	C <sub>27</sub> H <sub>31</sub> O <sub>16</sub>	491.1213, 403.1049, 325.0730	HSYA
Y3 <sup>a</sup>	23.04	359.0786	359.0761	6.96	C <sub>18</sub> H <sub>15</sub> O <sub>8</sub>	197.0462, 179.0356, 161.0249	Rosmarinic acid
Y4 <sup>a</sup>	23.67	537.1047	537.1027	3.72	C <sub>27</sub> H <sub>21</sub> O <sub>12</sub>	295.0621, 197.0463, 179.0354	Lithospermic acid
Y5 <sup>a</sup>	24.44	717.1502	717.1450	7.25	C <sub>36</sub> H <sub>29</sub> O <sub>16</sub>	519.0948, 339.0526, 321.0419	Salvianolic acid B

<sup>a</sup>: Components of the prototype. HSYA, hydroxysafflor yellow A.

**Danshensu-related metabolites.** At t<sub>R</sub> of 3.57 min, the excimer ion peak [M-H]<sup>-</sup> m/z 395.0949 in the negative ion mode of compound M2, with the molecular formula C<sub>18</sub>H<sub>19</sub>O<sub>10</sub>, fragment ions [M-H-C<sub>9</sub>H<sub>10</sub>O<sub>5</sub>]<sup>-</sup> m/z 197.0463 (C<sub>9</sub>H<sub>9</sub>O<sub>5</sub>), [M-H-C<sub>9</sub>H<sub>10</sub>O<sub>5</sub>-H<sub>2</sub>O]<sup>-</sup> m/z 179.0356 (C<sub>9</sub>H<sub>7</sub>O<sub>4</sub>), [M-H-C<sub>9</sub>H<sub>10</sub>O<sub>5</sub>-H<sub>2</sub>O-CO<sub>2</sub>]<sup>-</sup> m/z 135.0457 (C<sub>8</sub>H<sub>7</sub>O<sub>2</sub>). Its relative molecular mass increased by 197 Da (+C<sub>9</sub>H<sub>9</sub>O<sub>5</sub>) compared with that of danshensu, and based on its mass spectral information and secondary fragment ions, combined with the reference, it is assumed that compound M2 is a danshenin dimer [22]. At t<sub>R</sub> of 8.07 min, the excimer ion peak [M-H]<sup>-</sup> m/z 181.0484 in the negative ion mode of compound M4, with formula C<sub>8</sub>H<sub>9</sub>O<sub>4</sub>, and fragment ion [M-H-H<sub>2</sub>CO<sub>2</sub>]<sup>-</sup> m/z 135.0475 (C<sub>8</sub>H<sub>7</sub>O<sub>2</sub>), whose relative molecular mass is reduced by 16 Da (-O) compared to that of Danshensu, and according to reference, it is assumed that compound M4 is the deoxygenated product of Danshensu [23]. At t<sub>R</sub> 10.60 min, the [M-H]<sup>-</sup> molecular ion peak of compound M6 was m/z 277.0024. The molecular formula is C<sub>9</sub>H<sub>9</sub>O<sub>8</sub>S, and its fragment ion [M-H-SO<sub>3</sub>]<sup>-</sup> m/z 197.1301 (C<sub>8</sub>H<sub>7</sub>O<sub>2</sub>). The relative molecular mass is 80 Da, which is

more than the molecular weight of Danshensu. Combined with the literature, compound M6 is confirmed to be the sulfated binding product of Danshensu [24]. At t<sub>R</sub> of 22.81 min, the excimer ion peak [M-H]<sup>-</sup> m/z 245.0117 appeared in the negative ion mode for compound M9. The molecular formula is C<sub>9</sub>H<sub>9</sub>O<sub>6</sub>S (error 1.22), and the fragment ions [M-H-SO<sub>3</sub>]<sup>-</sup> m/z 165.0320, [M-H-SO<sub>3</sub>-CO<sub>2</sub>]<sup>-</sup> m/z 121.0302. The relative molecular mass of M9 is 32 Da less than that of M6. Combined with the relevant literature, it can be assumed that M9 is the product of double dehydroxylation and sulfation of Danshensu [25].

**HSYA related metabolites.** At t<sub>R</sub> of 20.51 min, the excimer ion peak [M-H]<sup>-</sup> m/z 593.1523 was observed in the negative ion mode for compound M8. The molecular formula is C<sub>27</sub>H<sub>29</sub>O<sub>15</sub>, and the fragment ion [M-H-C<sub>8</sub>H<sub>8</sub>O<sub>4</sub>]<sup>-</sup> m/z 472.9865 (C<sub>23</sub>H<sub>21</sub>O<sub>11</sub>), the relative molecular mass of M7 is reduced by 18 Da compared with that of hydroxysaffron yellow pigment A. Based on its mass spectral information and the secondary fragment ion, which is consistent with that reported in the literature, the compound M8 was identified as the dehydration



product of HSYA [26].

**Rosmarinic acid related metabolites.** At  $t_R$  of 20.51 min, the excimer ion peak  $[M-H]^-$   $m/z$  153.0192 ( $C_7H_5O_4$ ) appeared in the negative ion mode of compound M3. The fragment ions  $[M-H-CO_2]^-$   $m/z$  109.0223 ( $C_6H_5O_2$ ),  $[M-CO_2-H_2O]^-$   $m/z$  91.0194 ( $C_6H_5O$ ), which were checked against the control and combined with the literature, it is assumed that compound M4 is protocatechuic acid [27]. At  $t_R$  23.59 min, compound M13 showed excimer ion peak in negative ion mode  $[M-H]^-$   $m/z$  535.0893 ( $C_{27}H_{19}O_{12}$ ), fragment ions  $[M-H-C_9H_4O_4]^-$   $m/z$  359.0743 ( $C_{18}H_{15}O_8$ ),  $[M-H-C_9H_4O_4-C_9H_5O_3]^-$   $m/z$  197.0463 ( $C_9H_5O_5$ ),  $[M-H-H_2O-C_9H_4O_4-C_9H_5O_3]^-$   $m/z$  179.0354 ( $C_9H_7O_4$ ), whose relative molecular weight increased 176 Da compared with rosmarinic acid, and based on its mass spectral information and secondary fragment ions, combined with reference, it is assumed that compound M13 is a product of rosmarinic acid combined with glucuronic acid [28]. At a  $t_R$  of 30.03 min, compound M16 showed an excimer ion peak in negative ion mode  $[M-H]^-$   $m/z$  549.1077 ( $C_{25}H_{25}O_{14}$ ). The fragment ion  $[M-H-C_9H_4O_4]^-$   $m/z$  373.1106 ( $C_{16}H_{21}O_{10}$ ) and its relative molecular weight increased by 14 Da compared to M13, presumably resulting from further binding to a methyl group. Based on its mass spectral information and secondary fragmentation, combined with the literature, we therefore infer that M16 is the product of the combination of rosmarinic acid with a methyl group and glucuronic acid [29].

**Lithospermic acid related metabolites.** At  $t_R$  14.11 min, the excimer ion peak  $[M-H]^-$   $m/z$  551.1176 appeared in the negative ion mode of compound M7 with the molecular formula  $C_{28}H_{23}O_{12}$ . The fragment ions  $[M-H-H_2O]^-$   $m/z$  533.1116 ( $C_{28}H_{21}O_{11}$ ) and  $[M-H-CO_2]^-$   $m/z$  507.1337 ( $C_{27}H_{23}O_{10}$ ), the relative molecular mass of M7 increased by 14 Da compared to that of Lithospermic acid, and based on its mass spectral information and secondary fragment ions, which are consistent with those reported in the literature, compound M7 was identified as a post-methylation product of Lithospermic acid [30]. At  $t_R$  23.55 min, compound M12 showed an excimer ion peak  $[M-H]^-$   $m/z$  493.1152 ( $C_{26}H_{21}O_{10}$ ) in negative ion mode, and fragment ion  $[M-H-C_9H_{10}O_5]^-$   $m/z$  295.0620 ( $C_{17}H_{11}O_5$ ), whose relative molecular weight was reduced by 44 Da compared with that of Lithospermic acid. Based on the mass spectral information and the secondary fragment ions, it is assumed that compound M12 is a decarboxylated product of purpuric acid in combination with reference [31].

**Salvianolic acid B-related metabolites.** At  $t_R$  of 25.41 min, compound M15 showed an excimer ion peak  $[M-H]^-$   $m/z$  731.1607 ( $C_{37}H_{31}O_{16}$ ) in negative ion mode, the fragment ion  $[M-H-C_9H_{10}O_5]^-$   $m/z$  533.1100 ( $C_{28}H_{21}O_{11}$ ), whose exact molecular weight was increased by 14 Da (+CH<sub>3</sub>) compared with that of salvianolic acid B. Based on its mass spectral information and secondary fragment ions, compound M15 was presumed to be methyl salvianolic acid B [32].

In conclusion, by identifying and analyzing the metabolites of DHHP in the isolated intestinal flora of AMI rats, five prototypical components and 11 metabolites were obtained, and the specific chemical structures are shown in Figure 8.

#### Identification and analysis of metabolites of DHHP in the isolated intestinal flora of rats with AMI under inactivation conditions

Metabolism of rat intestinal incubation fluid was analyzed under inactivation conditions. At this experimental concentration, the primary components including Danshensu, Lithospermic acid, rosmarinic acid, HSYA, and salvianolic acid B were detected, while metabolites of other main components were not found.

#### Discussion

In recent years, there have been significant advances in biotechnology, including bioinformatics, metagenomic sequencing, and metabolomics. Numerous studies have demonstrated the inextricable link between the gut microbiome and cardiovascular diseases, as the former serves as a biological barrier that regulates host metabolic activity and modulates intestinal years [33]. In this study, metagenomic sequencing was employed to examine the intestinal

flora function trend in rats with AMI and the regulatory effect of the DHHP. The experiment revealed that the abundance and diversity of intestinal flora in rats were affected after establishing an AMI model. However, the DHHP successfully regulated the intestinal structure of AMI rats, thereby suppressing the intestinal disorders caused by AMI. *Escherichia* is a representative species that can cause infections of the gastrointestinal and urinary tracts, as well as local tissue and organs, in humans and various animals under specific conditions [34]. A study discovered that increased levels of glucose and lipid metabolism indicators and inflammatory factors in the coronary artery disease group were correlated with elevated abundance of *Escherichia* in the rat intestine [35]. Furthermore, research has demonstrated that *Escherichia* has the potential to contribute to atherosclerotic damage via TLR4-mediated oxidative stress [36]. *Butyricimonas*, a strictly anaerobic Gram-negative bacterium, was initially introduced by Sakamoto in 2009. Presently, there have been reports of five different *Butyricimonas* species, and several studies have indicated the significance of these species as key constituents of the fecal flora [37]. Only one of these species, *Butyricimonas virosa*, is considered pathogenic to date. Studies by Ulger Toprak N, Ogawa Y, Enemchukwu CU, and others have found that *Butyricimonas virosa* is present in all clinical cases of bacteremia related to peritonitis resulting from abdominal diseases [38, 39]. *Lactobacillus* is a probiotic commonly found in nature, with *Lactobacillus murinus* being one of the most prevalent strains. Numerous studies indicate that *Lactobacillus murinus* has demonstrated efficacy in treating colitis, hypertension, and intestinal ischemia, making it a potential probiotic that is commonly used [40, 41]. *Streptococcus* is an important pathogenic bacterium that can cause a variety of diseases in humans. Studies have shown that a high abundance of *Streptococcus* can be found in many cardiovascular diseases [42–44]. At the genus level, the relative abundance of *Parabacteroides*, *Butyricimonas*, *Odoribacter*, *Escherichia*, *Parasutterella* and other strains were significantly higher in the model rats of this study, and relative abundance of *Bacteroides* and *Lactobacillus* decreased significantly, indicating that the model was successfully established. While the DHHP has shown potential in significantly reversing abnormal strain levels, there is speculation that DHHP could inhibit toxin secretion by increasing probiotic bacteria levels and decreasing harmful bacteria levels in the intestines of rats within the AMI model. This, in turn, regulates the flora structure and ultimately improves the effect of myocardial ischemia.

Traditional Chinese medicine is predominantly administered orally, but some herbal medicines with good efficacy have low bioavailability when taken orally. This is closely linked to the intestinal flora [45]. At present, research has primarily focused on the metabolism of one active component of herbal medicines in the intestinal flora, whereas patients often take medications that contain multiple components [46]. Therefore, investigating the metabolites of multi-component Chinese medicines within the digestive tract microbiota and uncovering the interactions between microbiota and Chinese medicinal active ingredients can facilitate the development of novel Chinese medicine formulations and enhance the efficient employment of Chinese medicinal preparations [47]. In this study, the HPLC-Q-TOF-MS/MS technique was used to identify and analyze the metabolites of DHHP in the isolated intestinal bacterial fluid of AMI rats. At this concentration, a total of 16 metabolites were identified, including 5 progenitors, while no metabolites were detected in the inactivated rat intestinal incubate. The 11 metabolites mainly included the deoxygenated product of danshensu, a dimer of danshensu, sulfate product of danshensu, dehydrated product of HSYA, the decarboxylated product of Lithospermic acid and methylation product, glucuronidation product of rosmarinic acid and methylation product of tannic acid B. The determination of the metabolism of the active components of the DHHP in the isolated intestinal flora of AMI rats is tentatively established through experimental results. However, its ability to fully reflect the in vivo metabolic process of the active components is limited. Therefore, to fully reflect the metabolic process of the active components, it is indispensable to consider blood, bile, urine, and feces perspectives.

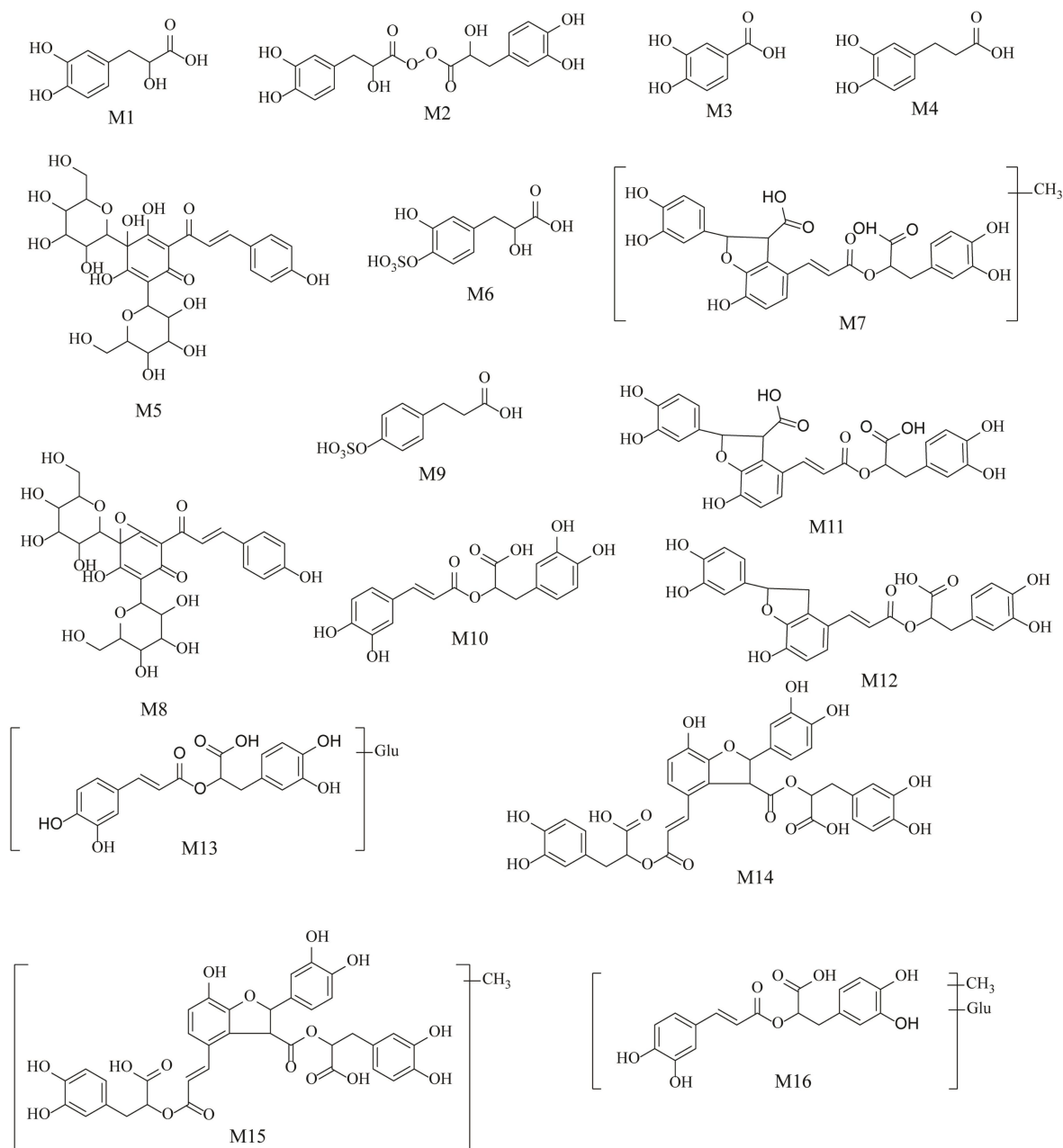


Figure 8 Structure of the metabolites

In summary, this study aimed to investigate the effect of DHHP on the intestinal flora of rats with AMI, as well as its in vitro microbiota transformation. The results suggest that there could be mutual regulation between DHHP and the intestinal flora. Moreover, further investigation is needed to see how the DHHP plays a therapeutic role after regulating the intestinal flora.

### Conclusion

The study indicates that DHHP considerably improves ISO-induced myocardial ischemia in rats with AMI. It also modifies the structural composition and relative abundance of intestinal flora. DHHP achieves its antimyocardial ischemic impact by fostering the growth of potential intestinal probiotics, like *Lactobacillus*, and hindering the growth of intestinal pathogens, such as *Escherichia* and *Streptococcus*. DHHP identified a total of 16 components, comprising 5 prototypes and 11 metabolites, in the intestinal bacterial cultures of model rats.

These metabolites were primarily generated through biotransformation pathways, such as methylation, hydroxylation and sulphation, deoxygenation, and dehydration. This study indicates the possibility of mutual regulation between DHHP and intestinal flora. It offers a valuable reference to clarify the forms of action of DHHP, pharmacodynamic pathways, and the development of novel drugs.

### References

1. Senthil S, Sridevi M, Pugalendi KV. Cardioprotective Effect of Oleanolic Acid on Isoproterenol-Induced Myocardial Ischemia in Rats. *Toxicol Pathol* 2007;35(3):418–423. Available at: <http://doi.org/10.1080/01926230701230312>
2. Tong JY, Zhang JB, Qin YF. Protective effect of activating luoxiaoling dan on acute injury in rats with myocardial ischemia. *Zhejiang J Chin Med* 2021;56(04):255–257. (Chinese) Available at:

- <http://doi.org/10.13633/j.cnki.zjtcn.2021.04.009>
3. He H, Zhou YB, Wang H, Ke R. Discussion on Relationship Between Intestinal Microflora and Ischemic Heart Disease Based on “Qi-Blood-Water”. *J Hunan Univ Chin Med* 2021;41(05):803–808. (Chinese) Available at: [https://kns.cnki.net/kcms2/article/abstract?v=jeDOxXNM7164tsLANkUOO2CulC8UUVS0Oiygg1FT61VT7\\_B2WD3YxY3WWIDf6xODHfYRpuZNVDiGh5WvVNWkPAWjRuLQONCm7yrW0dvofGS9XGWSABd7Dmw-k8uCos25n9PIS7ACIDho=&uniplatform=NZKPT&language=CHS](https://kns.cnki.net/kcms2/article/abstract?v=jeDOxXNM7164tsLANkUOO2CulC8UUVS0Oiygg1FT61VT7_B2WD3YxY3WWIDf6xODHfYRpuZNVDiGh5WvVNWkPAWjRuLQONCm7yrW0dvofGS9XGWSABd7Dmw-k8uCos25n9PIS7ACIDho=&uniplatform=NZKPT&language=CHS)
4. Tang WHW, Kitai T, Hazen SL. Gut Microbiota in Cardiovascular Health and Disease. *Circ Res* 2017;120(7):1183–1196. Available at: <http://doi.org/10.1161/CIRCRESAHA.117.309715>
5. Pu XH, Wang XY, Hao ZZ, Guo HW, Wang BM. Progress in the study of anti-myocardial ischemia of Saffron. *J Changchun Univ Chin Med* 2020;36(03):608–612. (Chinese) Available at: <http://doi.org/10.13463/j.cnki.cczyy.2020.03.057>
6. Shan XX, Hong BZ, Liu J, et al. [Review of chemical composition, pharmacological effects, and clinical application of *Salviae Miltiorrhizae Radix et Rhizoma* and prediction of its Q-markers]. *Zhongguo Zhong Yao Za Zhi* 2021;46(21):5496–5511. Available at: <http://doi.org/10.19540/j.cnki.cjcmm.20210630.203>
7. Zhou HH, Du SB, Gao S, Li J, Bai JQ, Wang XP. Optimisation of the preparation technique, TLC identification, and content determination of Danshen-Muscovite Dot Drop Granules. *West China J Pharm Sci* 2022;37(03):292–296. (Chinese) Available at: <http://doi.org/10.13375/j.cnki.wcjps.2022.03.014>
8. Hao CW, Li ZX, Zhang MH, Han B. Research progress of *Salvia miltiorrhiza* and its compatible preparations in treatment of coronary heart disease. *China Tradit Herb Drugs* 2021;52(13):4096–4106. (Chinese) Available at: [https://kns.cnki.net/kcms2/article/abstract?v=jeDOxXNM717D4SxaY1BgdtuDXFYFIBvMVHd7b\\_upJ\\_4RW\\_CW9Z-ZccDEqO\\_I\\_uMq93rU4-13R7Fb-zwaSIHdVFNmLp7qZw8nhxd09kOmaC6kSiRA4q-9YzB6jTxS-RRooeAT2SWtA4w=&uniplatform=NZKPT&language=CHS](https://kns.cnki.net/kcms2/article/abstract?v=jeDOxXNM717D4SxaY1BgdtuDXFYFIBvMVHd7b_upJ_4RW_CW9Z-ZccDEqO_I_uMq93rU4-13R7Fb-zwaSIHdVFNmLp7qZw8nhxd09kOmaC6kSiRA4q-9YzB6jTxS-RRooeAT2SWtA4w=&uniplatform=NZKPT&language=CHS)
9. Li WJ, Wang YP, Hong B. Study on the Mechanism of Honghua in Treatment of Myocardial Ischemia Based on Network Pharmacology. *World China Med* 2022;17(10):1371–1376. (Chinese) Available at: <https://kns.cnki.net/kcms2/article/abstract?v=jeDOxXNM714GPKMzcxeRAMDNtyOX4igMn1fuwMla5IuMmDGBfPohsiNpX5EUqk3hXikQXb14q9MVHF6dKDO0L8drHBOMc98tVP2jbAXJBgjF1Hq6V3v2F1--nrf3U8JzAegAaiYGitg=&uniplatform=NZKPT&language=CHS>
10. Zhou HH, Huan C, Xue ZP. HPLC-Q-TOF-MS/MS analysis of Danshen-Honghua herb pair in vivo metabolites in the intestinal flora. *Acta Pharm Sin* 2022;57(11):3371–3377. (Chinese) Available at: <http://doi.org/10.16438/j.0513-4870.2022-0589>
11. Gao LN, Cui YL, Yan K, Qiu C. Advances in studies on compatibility of *Salviae Miltiorrhizae Radix et Rhizoma* and *Carthamii Flos*. *China Tradit Herb Drugs* 2016;47(04):671–679. (Chinese) Available at: [https://kns.cnki.net/kcms2/article/abstract?v=jeDOxXNM717TNL9pYhL8RR9MXqAn9KDdP\\_onkBS-w\\_hJbdCPpOVOS3lcNoC8XVgIBI5NIEdWuEsCeUNod4ndkGGzAhk\\_Y-EdfklPnt3zdLJSCwRGU55rmkonwX1C7Of8PFCEXRA=&uniplatform=NZKPT&language=CHS](https://kns.cnki.net/kcms2/article/abstract?v=jeDOxXNM717TNL9pYhL8RR9MXqAn9KDdP_onkBS-w_hJbdCPpOVOS3lcNoC8XVgIBI5NIEdWuEsCeUNod4ndkGGzAhk_Y-EdfklPnt3zdLJSCwRGU55rmkonwX1C7Of8PFCEXRA=&uniplatform=NZKPT&language=CHS)
12. Han YP. Treatment of unstable angina pectoris with salvia polyphenolic acid salt and saffron yellow pigment the efficacy of angina pectoris. *Modern J Integr Tradit West Med (China)* 2010;19(08):943–944. (Chinese) Available at: [https://kns.cnki.net/kcms2/article/abstract?v=jeDOxXNM717dmtA8R5t2w4tDkpmcvOkFzLdJdVgzcKFEEGHm-z\\_j4\\_-NOH1Ev5JAWsGk0CJE0Hus8XHzcA\\_JqmPq416CTVFVcCaGg9rmh7Nwxw606DqPtTws1ujeQoxgNd&uniplatform=NZKPT&language=CHS](https://kns.cnki.net/kcms2/article/abstract?v=jeDOxXNM717dmtA8R5t2w4tDkpmcvOkFzLdJdVgzcKFEEGHm-z_j4_-NOH1Ev5JAWsGk0CJE0Hus8XHzcA_JqmPq416CTVFVcCaGg9rmh7Nwxw606DqPtTws1ujeQoxgNd&uniplatform=NZKPT&language=CHS)
13. Bi C, Li PL, Liao Y, et al. Pharmacodynamic effects of Dan-hong injection in rats with blood stasis syndrome. *Biomed Pharmacother* 2019;118:109187. Available at: <http://doi.org/10.1016/j.biopha.2019.109187>
14. Yang G, He HQ, Chen G, Wang J. Effect of traditional Chinese medicine in attenuating coronary heart disease and main risk factors by regulating gut micro-biota. *Zhongguo Zhong Yao Za Zhi* 2020;45(1):29–36. Available at: <http://doi.org/10.19540/j.cnki.cjcmm.20190505.502>
15. Deng J, Tang M, Wen HB, Cao YC. Molecular Mechanisms of Cardioprotective Effects of Resveratrol. *Medical Recapitulate. Med Recapitulate* 2018;24(14):2759–2764. (Chinese) Available at: [https://kns.cnki.net/kcms2/article/abstract?v=jeDOxXNM7140UbU3Kq1AuNqPMjYcCtjSOIRoqrCDNEWB07I-2k2grcbdaz55G-J0y\\_-BafY3g8fXEultZLqrNcMYjccyIDLTVQN3BtaqTE\\_PfUqQnRW9vi7y-YT5RdtHtdreR-MzTdc=&uniplatform=NZKPT&language=CHS](https://kns.cnki.net/kcms2/article/abstract?v=jeDOxXNM7140UbU3Kq1AuNqPMjYcCtjSOIRoqrCDNEWB07I-2k2grcbdaz55G-J0y_-BafY3g8fXEultZLqrNcMYjccyIDLTVQN3BtaqTE_PfUqQnRW9vi7y-YT5RdtHtdreR-MzTdc=&uniplatform=NZKPT&language=CHS)
16. Feng Q, Liu W, Baker SS, et al. Multi-targeting therapeutic mechanisms of the Chinese herbal medicine QHD in the treatment of non-alcoholic fatty liver disease. *Oncotarget* 2017;8(17):27820–27838. Available at: <http://doi.org/10.18632/oncotarget.15482>
17. Ghosh SS, Bie J, Wang J, Ghosh S. Oral supplementation with non-absorbable antibiotics or curcumin attenuates western diet-induced atherosclerosis and glucose intolerance in LDLR-/- mice—role of intestinal permeability and macrophage activation. *PLoS One* 2014;9(9):e108577. Available at: <http://doi.org/10.1371/journal.pone.0108577>
18. Li Q, Guo Y, Yu X, Liu W, Zhou L. Protective mechanism of rhubarb anthraquinone glycosides in rats with cerebral ischaemia–reperfusion injury: interactions between medicine and intestinal flora. *Chin Med* 2020;15(1):60. Available at: <http://doi.org/10.1186/s13020-020-00341-x>
19. Yang B, Fan Z, Zhao L, et al. In vitro metabolic transformation of syringin by rat intestinal flora. *China Tradit Herb Drugs* 2015;46(09):1333–1337. (Chinese) Available at: [https://kns.cnki.net/kcms2/article/abstract?v=jeDOxXNM716tBfuixfeCjKPW89qLEbHF4TPlw8ZU\\_D7FA\\_M5GoQjmGWgyC7ymZ\\_iYVMkodPiv8GzQB3UaZ0gGTTvyTn5mSTYiu1nR08Q5XNCzciwCs90T\\_7OexxqRyli--NPWPYKA=&uniplatform=NZKPT&language=CHS](https://kns.cnki.net/kcms2/article/abstract?v=jeDOxXNM716tBfuixfeCjKPW89qLEbHF4TPlw8ZU_D7FA_M5GoQjmGWgyC7ymZ_iYVMkodPiv8GzQB3UaZ0gGTTvyTn5mSTYiu1nR08Q5XNCzciwCs90T_7OexxqRyli--NPWPYKA=&uniplatform=NZKPT&language=CHS)
20. Huang ML, Song HP, Pang HQ, Gao W, Wen XD. Research progress of the pharmacokinetics of safflor yellow pigments. *Pharm Clin Res* 2018;26(04):287–290. (Chinese) Available at: <http://doi.org/10.13664/j.cnki.pcr.2018.04.012>
21. Yuan CP, Hou HM, Qu SY. Progress in the pharmacokinetics and relative studies of salvianolic acid B. *Chin New Drugs J* 2015;24(07):791–799. (Chinese) Available at: <https://kns.cnki.net/kcms/detail/11.2850.R.20150417.1440.014.html>
22. Zhao X, Yang D, Xu F, et al. The in vivo absorbed constituents and metabolites of Danshen decoction in rats identified by HPLC with electrospray ionization tandem ion trap and time-of-flight mass spectrometry. *Biomed Chromatogr* 2014;29(2):285–304. Available at: <http://doi.org/10.1002/bmc.3275>
23. Gu J, Feng L, Zhang M, et al. New metabolite profiles of Danshensu in rats by ultraperformance liquid chromatography/quadrupole-time-of-flight mass spectrometry. *J Chromatogr B Analyt Technol Biomed Life Sci* 2014;955–956:20–25. Available at: <http://doi.org/10.1016/j.jchromb.2014.02.010>
24. Pang H, Jiang M, Wang Q, et al. Metabolic profile of danshen in rats by HPLC-LTQ-Orbitrap mass spectrometry. *J Zhejiang Univ Sci B* 2018;19(3):227–244. Available at: <http://doi.org/10.1631/jzus.B1700105>
25. Mei XD, Wang YQ, Wang ZJ, et al. Identification of metabolites

- of Danshensu in vivo in rats. *Zhongguo Zhong Yao Za Zhi* 2018;43(19):3933–3939. (Chinese) Available at: <http://doi.org/10.19540/j.cnki.cjcmm.20180709.010>
26. Wu L, Tang Y, Shan C, et al. A comprehensive in vitro and in vivo metabolism study of hydroxysafflor yellow A. *J Mass Spectrom* 2017;53(2):99–108. Available at: <http://doi.org/10.1002/jms.4041>
  27. Guo HM, Su ZY, Gao SK, Du Y, Ji S, Tang DQ. Analysis of in vivo metabolites of Compound Danshen Dripping Pills in rats. *China Tradit Patent Med* 2019;41(10):2307–2314. (Chinese) Available at: [https://kns.cnki.net/kcms2/article/abstract?v=jeDOxXNM7I7cMJJO\\_aFPxT3vYwBZ96V\\_M7dmDy2rG6W2PUxhbsgzLWLGDCycXl2uYVIL2bzSYnj5huE9yUwYbGoeM\\_wXUNrAZx7SPFdNHZJapvTNfM0o-mK0\\_lklqKy23zNxBc8sQ=&uniplatform=NZKP T&language=CHS](https://kns.cnki.net/kcms2/article/abstract?v=jeDOxXNM7I7cMJJO_aFPxT3vYwBZ96V_M7dmDy2rG6W2PUxhbsgzLWLGDCycXl2uYVIL2bzSYnj5huE9yUwYbGoeM_wXUNrAZx7SPFdNHZJapvTNfM0o-mK0_lklqKy23zNxBc8sQ=&uniplatform=NZKP T&language=CHS)
  28. Sun SF. Study on the metabolism of active ingredient rosmarinic acid in *Salvia miltiorrhiza*. *Heilongjiang Univ Tradit Chin Med* 2009. (Chinese) Available at: [https://kns.cnki.net/kcms2/article/abstract?v=jeDOxXNM7I6sODZbozuE2xnp\\_Klx8O6fBF1ATBGafz0vshuctUh1MKjZv\\_QxYHIYYGprZPRCMF7pHQhNxR3KkjsBttPpK01GTAAwUwLjjDqr3vcDCEetHTqLw4q6aTGr&uniplatform=NZKPT&language=CHS](https://kns.cnki.net/kcms2/article/abstract?v=jeDOxXNM7I6sODZbozuE2xnp_Klx8O6fBF1ATBGafz0vshuctUh1MKjZv_QxYHIYYGprZPRCMF7pHQhNxR3KkjsBttPpK01GTAAwUwLjjDqr3vcDCEetHTqLw4q6aTGr&uniplatform=NZKPT&language=CHS)
  29. Guo SB, Xu LL, Jiang LJ, et al. Profiling and identification of in vivo metabolism of rosmarinic acid in rats. *Zhongguo Zhong Yao Za Zhi* 2019 Nov;44(21):4704–4712. (Chinese) Available at: <http://doi.org/10.19540/j.cnki.cjcmm.20190314.001>
  30. Hou MN, Gu X, Xie Z. Study on metabolites and metabolic pathway of salvianolic acid B in rats. *Chin J Mod Appl Pharm*. *Chin J Mod Appl Pharm* 2019;36(21):2673–2682. (Chinese) Available at: <http://doi.org/10.13748/j.cnki.issn1007-7693.2019.21.009>
  31. Wang L, Zhang Q, Li X, et al. Pharmacokinetics and metabolism of lithospermic acid by LC/MS/MS in rats. *Int J Pharm* 2008;350(1–2):240–246. Available at: <http://doi.org/10.1016/j.ijpharm.2007.09.001>
  32. Zeng G, Xiao H, Liu J, Liang X. Identification of phenolic constituents in *Radix Salvia miltiorrhizae* by liquid chromatography/electrospray ionization mass spectrometry. *Rapid Comm Mass Spectrometry* 2006;20(3):499–506. Available at: <http://doi.org/10.1002/rcm.2332>
  33. Du S-B, Zhou H-H, Wang P-F, et al. Modulation effects of danshen-honghua herb pair on gut microbiota of acute myocardial ischemia model rat. *FEMS Microbiol Lett* 2022;369(1):fnac036. Available at: <http://doi.org/10.1093/femsle/fnac036>
  34. Yin ZL, Wan H. A review of studies on *Escherichia coli*. *Gansu Animal Husbandry and Veterinary* 2019;49(05):33–35. Available at: <http://doi.org/10.15979/j.cnki.cn62-1064/s.2019.05.010>
  35. Peng Y, Zhang N, Li WJ, et al. Correlations of changes in inflammatory factors, glucose and lipid metabolism indicators and adiponectin with alterations in intestinal flora in rats with coronary heart disease. *Eur Rev Med Pharmacol Sci* 2020;24(19):10118–10125. Available at: [http://doi.org/10.26355/eurev\\_202010\\_23231](http://doi.org/10.26355/eurev_202010_23231)
  36. Carnevale R, Nocella C, Petrozza V, et al. Localization of lipopolysaccharide from *Escherichia Coli* into human atherosclerotic plaque. *Sci Rep* 2018;8(1):3598. Available at: <http://doi.org/10.1038/s41598-018-22076-4>
  37. García-Agudo L, Nilsen E. *Butyricimonas virosa*: A rare cause of bacteremia. *Anaerobe* 2018;54:121–123. Available at: <http://doi.org/10.1016/j.anaerobe.2018.08.001>
  38. Ulger Toprak N, Bozan T, Birkan Y, Isbir S, Soyletir G. *Butyricimonas virosa*: the first clinical case of bacteraemia. *New Microbes New Infect* 2015;4:7–8. Available at: <http://doi.org/10.1016/j.nmni.2014.12.004>
  39. Ogawa Y, Sato M, Yamashita T, et al. Polymicrobial Anaerobic Bacteremia Caused by *Butyricimonas virosa* and *Brachyspira pilosicoli* in a Patient with Peritonitis following Intestinal Perforation. *Ann Lab Med* 2018;38(1):71–73. Available at: <http://doi.org/10.3343/alm.2018.38.1.71>
  40. Hu J, Deng F, Zhao B, et al. *Lactobacillus murinus* alleviate intestinal ischemia/reperfusion injury through promoting the release of interleukin-10 from M2 macrophages via Toll-like receptor 2 signaling. *Microbiome* 2022;10(1):38. Available at: <http://doi.org/10.1186/s40168-022-01227-w>
  41. Isani M, Bell BA, Delaplain PT, et al. *Lactobacillus murinus* HF12 colonizes neonatal gut and protects rats from necrotizing enterocolitis. *PLoS One* 2018;13(6):e0196710. Available at: <http://doi.org/10.1371/journal.pone.0196710>
  42. Ott SJ, El Mokhtari NE, Musfeldt M, et al. Detection of Diverse Bacterial Signatures in Atherosclerotic Lesions of Patients With Coronary Heart Disease. *Circulation* 2006;113(7):929–937. Available at: <http://doi.org/10.1161/CIRCULATIONAHA.105.579979>
  43. Jie Z, Xia H, Zhong SL, et al. The gut microbiome in atherosclerotic cardiovascular disease. *Nat Commun* 2017;8(1):845. Available at: <http://doi.org/10.1038/s41467-017-00900-1>
  44. Renvert S, Pettersson T, Ohlsson O, Persson GR. Bacterial Profile and Burden of Periodontal Infection in Subjects With a Diagnosis of Acute Coronary Syndrome. *J Periodontol* 2006;77(7):1110–1119. Available at: <http://doi.org/10.1902/jop.2006.050336>
  45. Men W, Chen Y, Li YJ, et al. Research Progress of Biotransformation on Effective Ingredients of Chinese Medicine Via Intestinal Bacteria. *China J Experimental Tradit Med Formulae* 2015;21(02):229–234. (Chinese) Available at: <http://doi.org/10.13422/j.cnki.syfx.2015020229>
  46. Cui Q, Pan Y, Xu X, et al. The metabolic profile of acteoside produced by human or rat intestinal bacteria or intestinal enzyme in vitro employed UPLC-Q-TOF-MS. *Fitoterapia* 2016;109:67–74. Available at: <http://doi.org/10.1016/j.fitote.2015.12.011>
  47. Chen H, Wang CQ, Xia T, et al. Analysis of in Vitro Metabolic Characteristics of Effective Components of *Polygonum orientale* Flower in Human Intestinal Flora. *Nat Prod Res Dev* 2018;30(12):2097–2103 + 2062. (Chinese) Available at: <http://doi.org/10.16333/j.1001-6880.2018.12.010>